International Journal of Environmental Impacts
https://www.acadlore.com/journals/IJEI

Multi-Decadal Shoreline Dynamics and Pathways for Sustainable Coastal Management in Ujung Pangkah, Indonesia

Andik Isdianto[1,2*], Ilham Maulana Asyari[2], Dhira Khurniawan Saputra[2], Rudianto[2], Arief Setyanto[2], Tri Djoko Lelono[2], Gatut Bintoro[2], Qurrota A'Yun[2], Uun Yanuhar[3], Nico Rahman Caesar[3], Aulia Lanudia Fathah[4], Alifiulahtin Utaminingsih[5], Mohammad Maskan[6], Berlania Mahardika Putri[7], Dwi Candra Pratiwi[8]

[1] Master Program of Leadership and Policy Innovation, Brawijaya University, 65145 Malang, Indonesia
[2] Department of Fishery and Marine Resources Utilization, Brawijaya University, 65145 Malang, Indonesia
[3] Department of Fisheries Marine Resources Management, Brawijaya University, 65145 Malang, Indonesia
[4] Master Program of Environmental Management and Development, Brawijaya University, 65145 Malang, Indonesia
[5] Doctoral Program in Sociology, Brawijaya University, 65145 Malang, Indonesia
[6] Department of Business Administration, State Polytechnic of Malang, 65141 Malang, Indonesia
[7] Master Program of Environmental Science, Graduate School of Universitas Gadjah Mada, 55284 Yogyakarta, Indonesia
[8] Earth and Atmospheric Sciences Department, University of Alberta, T6G 2E3 Edmonton, Canada

[*] Correspondence: Andik Isdianto (andik.isdianto@ub.ac.id)

Received: 08-28-2025 **Revised:** 11-21-2025 **Accepted:** 02-13-2026

Citation: A. Isdianto, I. M. Asyari, D. K. Saputra, Rudianto, A. Setyanto, T. D. Lelono, G. Bintoro, Q. A'Yun, U. Yanuhar, N. R. Caesar, A. L. Fathah, A. Utaminingsih, M. Maskan, B. M. Putri, and D. C. Pratiwi, "Multi-decadal shoreline dynamics and pathways for sustainable coastal management in Ujung Pangkah, Indonesia ," *Int. J. Environ. Impacts.*, vol. 9, no. 3, pp. 769–783, 2026. https://doi.org/10.56578/ijei090312.

Abstract: Shoreline change strongly affects ecosystem conditions and livelihood security in deltaic coasts. However, long-term and spatially explicit baselines remain limited for many rapidly changing coastal systems. This study quantified multi-decadal shoreline dynamics in Ujung Pangkah, Indonesia, to identify persistent patterns of accretion and erosion and to assess their implications for sustainable coastal management. Multi-epoch satellite images from 1973 to 2021 were used to extract shoreline positions through water-index-based classification. The extracted shorelines were analyzed using standardized Digital Shoreline Analysis System (DSAS) metrics to estimate net shoreline movement (NSM) and end point rate (EPR) across segmented coastal areas. The results indicate a segment-structured shoreline mosaic rather than a uniform coast-wide trend. Most sectors were accretion-dominated, with the accretion component reaching approximately +12 to +15 m·yr^{-1}, particularly in Area C. In contrast, Area D formed the main erosional hotspot, with an erosion component of -8.68 m·yr^{-1} and an NSM erosion value of -416.53 m, while its net EPR and net NSM were -0.66 m·yr^{-1} and -31.77 m, respectively. These findings show that shoreline change in Ujung Pangkah is spatially concentrated in localized reaches. Therefore, coast-wide averages may obscure areas where erosion risk persists and where accretion gains are sustained. This study provides a quantitative long-term baseline and a reproducible remote-sensing and GIS-based workflow to support hotspot identification, segment-scale monitoring, and the prioritization of coastal protection and rehabilitation measures in dynamic deltaic environments.

Keywords: Shoreline change; Digital Shoreline Analysis System; Net shoreline movement; End point rate; Coastal erosion; Coastal accretion; Deltaic coast; Sustainable coastal management

1 Introduction

Coastlines are dynamic land–sea interfaces shaped by waves, tides, currents, sediment supply, and human activities. These processes generate spatially variable patterns of erosion and accretion. In deltaic settings, shoreline dynamics are often more complex because fluvial sediment inputs, monsoon-driven circulation, and low coastal gradients interact over time [1, 2]. Ujung Pangkah, located at the mouth of the Bengawan Solo River in Indonesia, represents this type of dynamic deltaic coast. Previous studies have reported high variability in currents, suspended sediment transport, and shoreline responses along the Gresik–Madura Strait corridor [3, 4]. These changes have direct implications

for mangrove condition, fisheries production, aquaculture viability, and coastal community resilience. Therefore, reliable long-term shoreline monitoring is needed to support sustainable coastal planning, conservation, and livelihood protection [5, 6].

Satellite-based Earth observation provides a practical basis for detecting shoreline change over long time periods. Multi-epoch satellite imagery can be combined with water–land separation indices, such as the Normalized Difference Water Index (NDWI) and Modified Normalized Difference Water Index (MNDWI), to extract shoreline positions consistently. When these shoreline datasets are analyzed using the Digital Shoreline Analysis System (DSAS), they can provide standardized measurements of shoreline displacement and change rates across different coastal segments [7]. However, shoreline metrics alone are insufficient for management interpretation. They need to be evaluated together with hydro-morphological conditions, including tides, waves, currents, and coastal slope, to identify possible drivers and intervention priorities [8].

Despite the environmental and socio-economic importance of Ujung Pangkah, a unified multi-decadal baseline of shoreline change remains limited. Existing information has not fully integrated long-term satellite-derived shoreline positions, DSAS-based change metrics, hydro-oceanographic interpretation, and land-use context into a single management-oriented assessment. This gap limits the ability to distinguish persistent erosion hotspots from areas where accretion has been sustained. It also constrains the translation of shoreline-change evidence into segment-specific coastal management strategies.

This study addresses this gap by quantifying multi-decadal shoreline dynamics in Ujung Pangkah from 1973 to 2021. The analysis aims to: (i) establish a long-term shoreline baseline across the satellite era; (ii) identify spatial patterns of accretion and erosion using DSAS metrics; (iii) interpret these patterns in relation to hydro-oceanographic conditions and land-use change; and (iv) translate the results into management pathways for coastal protection, mangrove rehabilitation, and sustainable coastal planning. Two hypotheses are tested. First, shoreline change in Ujung Pangkah is organized into accretionary and erosional cells rather than forming a uniform coast-wide trend. Second, accreting sectors are associated with conditions that favor sediment retention and mangrove stabilization, whereas persistent erosion is linked to stronger hydrodynamic exposure and reduced sediment trapping [5, 9].

This study argues that integrating multi-decadal satellite-derived shorelines, DSAS metrics, hydro-oceanographic context, and land-use information can reveal whether shoreline change in Ujung Pangkah forms a uniform trend or a segment-structured erosion–accretion mosaic. By applying this workflow to the 1973–2021 shoreline record, the study provides a long-term spatial baseline, identifies priority erosion and accretion sectors, and translates the results into management pathways for mangrove rehabilitation, coastal protection, and spatial-planning integration. This contribution supports evidence-based coastal management in Ujung Pangkah and provides a reproducible approach for other deltaic environments facing similar shoreline-change dynamics.

2 Methodology

2.1 Study Area

Ujung Pangkah District is located in Gresik Regency, East Java, Indonesia, and covers approximately 9,483.23 ha across 13 villages. The area is predominantly low-lying and forms part of a dynamic deltaic coast influenced by the Bengawan Solo River. This study analyzed approximately 30 km of coastline. The coastline was divided into six 5-km analysis areas based on coastal profile characteristics and extreme net shoreline movement (NSM) values. The western and eastern coastal sectors, represented by Pangkah Kulon and Pangkah Wetan, are shown in Figure 1. The station names, representative coordinates, DSAS areas, and brief descriptions are listed in Table 1.

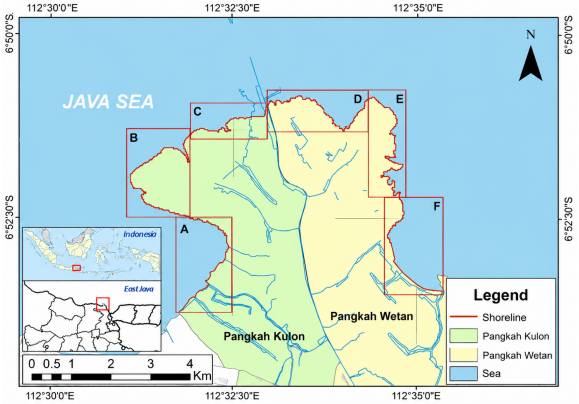

Figure 1. Study area and Digital Shoreline Analysis System (DSAS) analysis domains in Ujung Pangkah, Gresik Regency

Table 1. Division of research areas (A–F) and representative station coordinates

Station	Coordinate		Area (DSAS)	Description
	Longitude (°E)	Latitude (°S)		
Pangkah Kulon				
1	112.313°	6.533°	A	Dominated by pond areas
2	112.321°	6.525°	B	Dominated by mangrove areas
3	112.312°	6.522°	C	Located in the estuary areas
Pangkah Wetan				
4	112.311°	6.513°	D	Located in the estuary areas
5	112.325°	6.513°	E	Dominated by mangrove areas
6	112.341°	6.505°	F	Dominated by pond areas

Note: DSAS, Digital Shoreline Analysis System.

The stations served as reference points for the six DSAS analysis areas along the Ujung Pangkah coastline. Coordinates are reported in decimal degrees. The area codes A–F correspond to the analysis domains shown in Figure 1 and are used consistently throughout the shoreline-change analysis.

2.2 Data Sources and Collection

This study used secondary datasets to quantify shoreline change and interpret the physical and land-use context of coastal dynamics. The datasets, providers, access points, and analytical roles are summarized in Table 2. The analytical workflow consisted of shoreline extraction from Landsat imagery, DSAS-based calculation of shoreline-change metrics, and contextual interpretation using tidal, wave, current, beach-slope, and land-use datasets.

Table 2. Data collection overview

No.	Dataset	Product	Role in This Study	Used in Step/Section
1	Satellite imagery (30 m)	Landsat 1, 3, 5 TM Landsat 7 ETM+ Landsat 8 OLI USGS Glovis (http://glovis.usgs.gov/app)	Extract multi-epoch shorelines (MNDWI/threshold) for DSAS (1973–2021)	Shoreline extraction; DSAS (Methodology 2.3–2.5; Results 3.3–3.4)
2	Tides	Tides BIG (http://tides.big.go.id)	Tidal normalization/reference water level for shoreline interpretation	Tidal normalization (Methodology 2.5; Results 3.1)
3	Waves	Copernicus (https://cds.climate.copernicus.eu)	Physical forcing context to interpret exposure/erosion–accretion patterns (not used to compute DSAS rates)	Forcing context (Methodology 2.6; Results 3.1; Discussion 4.2)
4	Ocean currents	NASA PODAAC (http://podaac.jpl.nasa.gov)	Alongshore transport context to interpret spatial mosaics (not used to compute DSAS rates)	Forcing context (Methodology 2.7; Results 3.1; Discussion 4.2)
5	Beach slope	DEMNAS (https://tanahair.indonesia.go.id/demnas)	Estimate gentle coastal slope as coastal setting parameter	Beach slope (Methods 2.8; Results 3.2)
6	Indonesian Topographic Map	Indonesian Geospatial Portal (http://tanahair.indonesia.go.id)	Cartography only (study area map, administrative context)	Maps (Methodology 2.1; Results 3.3)
7	Land use (30 m)	USGS Glovis (http://glovis.usgs.gov/app)	Produce land-use dynamics table; interpret anthropogenic drivers	Land-use dynamics (Methodology 2.9; Results 3.3)

Note: DSAS, Digital Shoreline Analysis System.

Multi-epoch Landsat imagery was used as the primary dataset for shoreline extraction and DSAS analysis. The shoreline epochs included 1973, 1982, 1994, 1996, 2001, 2006, 2011, 2016, and 2021. Tidal data were used to support tidal normalization and shoreline interpretation. Wave, ocean-current, beach-slope, and land-use datasets were not used to compute DSAS rates directly. Instead, these datasets provided interpretative context for explaining spatial differences in erosion and accretion patterns across the study area.

2.3 Satellite Imagery Pre-Processing and Shoreline Extraction

Satellite imagery was pre-processed in ENVI 5.1 before shoreline extraction. The pre-processing steps included geometric, radiometric, and atmospheric corrections. Atmospheric correction was performed using the Fast

Line-of-sight Atmospheric Analysis of Spectral Hypercubes (FLAASH) module.

Because the Landsat sensor configurations differed across the observation period, sensor-consistent water indices were applied. The Normalized Difference Water Index (NDWI) was used for Landsat MSS imagery from 1973 and 1982. The Modified Normalized Difference Water Index (MNDWI) was used for Landsat TM, ETM+, and OLI imagery from 1994 to 2021 [10, 11]. MNDWI uses the shortwave infrared band instead of the near-infrared band and generally improves land–water separation. Scene-specific thresholds were then applied using Otsu classification and visual refinement. The resulting water masks were vectorized to generate shoreline positions. Quality control included visual inspection against true-color composites and morphological cleaning of the extracted shoreline features.

2.4 Digital Shoreline Analysis System and Uncertainty

Shoreline-change statistics were computed using the DSAS v4.3 with a baseline–transect approach [12]. All shoreline epochs listed in Table 2 were merged into a single shoreline feature class. A shore-parallel baseline was digitized using the study-area frame shown in Figure 1. From this baseline, 451 shore-normal transects were generated to sample shoreline displacement across the six analysis areas. The primary end-point metrics are:

(1) NSM (end-point displacement), defined as the end-point displacement between the youngest and oldest shoreline for each transect.

$$\text{NSM} = \text{Distance}\left(\text{Oldest shoreline} - \text{Youngest shoreline}\right) \tag{1}$$

(2) End point rate (EPR), the annualised rate computed as

$$\text{EPR} = \frac{\text{NSM}}{\Delta \text{T}} \tag{2}$$

where, T represents 48 years for 1973–2021.

For additional context, the Linear Regression Rate (LRR) was considered as an indicator of longer-term shoreline tendency. Shoreline-change magnitudes were classified following [12, 13] into high accretion (>4 m·yr^{-1}), low accretion (1–4 m·yr^{-1}), stable shoreline position (-1 to 1 m·yr^{-1}), low erosion (-4 to -1 m·yr^{-1}), and high erosion (<-4 m·yr^{-1}). Quality control followed standard DSAS procedures. Shoreline positions were co-registered and interpreted using consistent tidal-stage information. Therefore, NSM and EPR values were interpreted with caution in relation to the 30-m spatial resolution of Landsat imagery and tidal-normalization uncertainty.

2.5 Tides and Tidal Normalization

Tidal predictions from the Indonesian Geospatial Information Agency were used to guide image selection and shoreline interpretation. Where possible, satellite scenes were selected under similar tidal-stage conditions. When tidal stages differed, shoreline positions were interpreted relative to a common reference level using predicted tidal levels at the satellite overpass time. The tidal regime was described using the Formzahl number, and mean sea level was used as the reference datum [14]. These tidal data supported shoreline interpretation and uncertainty control but were not used as direct inputs for DSAS rate computation.

2.6 Waves

Wave and wind data from Copernicus were cropped to the study area and used to describe seasonal wave-forcing conditions. The data were transformed into effective fetch, and significant wave height (Hs) and peak wave period (Tp) were estimated using the Simplified Manning–Boussinesq formulation [15]. Seasonal and representative monthly wave conditions were summarized to support interpretation of potential longshore transport and erosion–accretion patterns. These wave data provided physical-forcing context and were not used to compute NSM or EPR values.

2.7 Ocean Currents

Surface-current data from the NASA Physical Oceanography Distributed Active Archive Center (PO.DAAC) were processed in Surfer 10.1 [16]. The processing generated annual means, seasonal composites, and a November snapshot to support interpretation of sediment-transport pathways. The resulting vector and contour maps were used to identify potential zones of sediment convergence and divergence. These current data were used as interpretative evidence for explaining shoreline-change patterns and were not used directly in DSAS calculations.

2.8 Coastal Topography and Beach Slope

Digital Elevation Model Nasional (DEMNAS) data were clipped to the coastal corridor and buffered to 1 km inland [17]. Beach slope was calculated in degrees and averaged for each analysis area. The slope values were used to characterize coastal profile conditions and to support interpretation of shoreline response. They were not used to compute shoreline-change rates.

2.9 Land Use

Landsat-derived land-use data were clipped to the study boundary, radiometrically corrected, and sharpened where applicable. Unsupervised classification was used to classify land use into settlement, rice fields, ponds, vegetation, and rivers [18]. The classified maps were used to summarize land-use dynamics across the study period. In the main analysis, percentage values were emphasized because they are more robust to differences in mapping extent. Absolute area values in hectares were reported as supporting information after checking the consistency of study-area clipping and unit conversion. Land-use information was used to interpret possible anthropogenic drivers of shoreline change, not to calculate DSAS shoreline-change metrics.

3 Results

3.1 Physical Forcing and Coastal Setting (Currents, Waves, Tides, and Beach Slope)

Seasonal surface currents in Ujung Pangkah ranged from approximately 0.015 to 0.37 $m \cdot s^{-1}$ and generally moved from west to east (Figure 2). During the East Monsoon, winds from Australia toward Asia reinforced the eastward flow. During the West Monsoon, the circulation became more variable and could redirect local current patterns. These seasonal current patterns indicate that monsoon-driven circulation may influence alongshore sediment redistribution and shoreline response in northern Java [19].

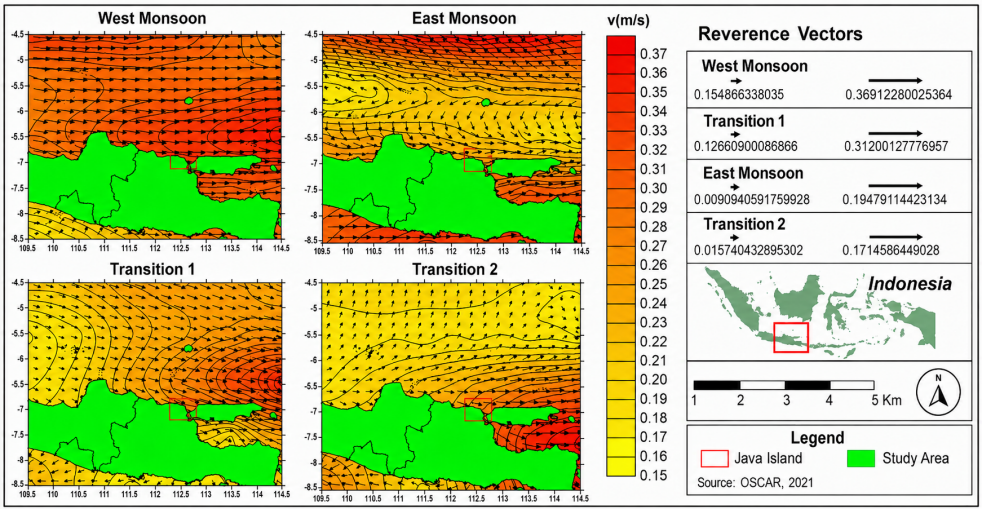

Figure 2. Maps of ocean current velocity and direction based on seasons

Wave conditions also varied seasonally (Figure 3). Significant wave height showed relatively small seasonal variation, whereas peak wave period varied more strongly among the West Season, East Season, Transition Season 1, and Transition Season 2. Periods of stronger seasonal forcing and large-scale climate anomalies may increase wave energy and raise the potential for shoreline retreat in exposed coastal reaches [19].

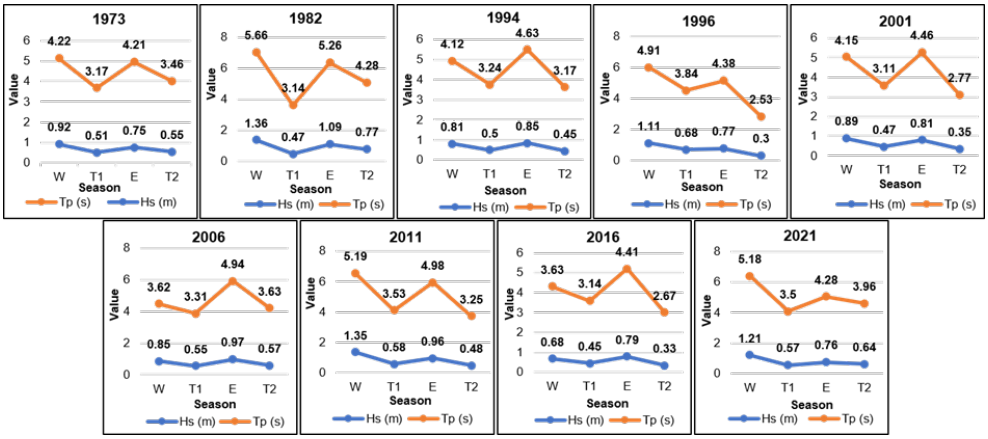

Figure 3. Wave height and wave period (1973–2021) in Ujung Pangkah—West Season (W); East Season (E); Transition Season 1 (T1); and Transition Season 2 (T2)

The tidal regime was diurnal, with a Formzahl value of approximately 7.64 (Figure 4). Sea-level interpretation in this study was based on the analysis datum, with mean sea level used as the reference level. Extreme high tides may temporarily shift the observed waterline and expand inland inundation, thereby influencing short-term shoreline position [20].

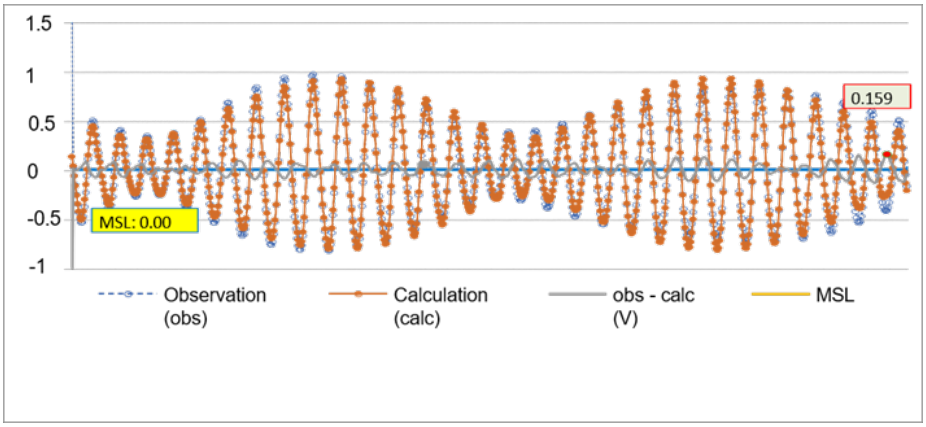

Figure 4. Ujung Pangkah tide prediction chart

Beach slopes were very gentle across all analysis areas, ranging from 0.02° to 0.05° over a 1,000 m inland distance, with an overall mean of approximately 0.04° (Table 3). These low-gradient profiles favor energy dissipation and provide accommodation space for sediment deposition where sediment supply is sufficient.

Table 3. Ujung Pangkah beach slope (November 2021)

Area	Measurement Distance (m)	Avg. Slope (°)
A	1000	0.04
B	1000	0.04
C	1000	0.05
D	1000	0.05
E	1000	0.04
F	1000	0.02
Overall mean		**0.04**

3.2 Land-Use Dynamics from 1973 to 2021

Land use was classified into settlement, rice fields, ponds, vegetation, and rivers (Table 4 and Table 5). Over the 1973–2021 period, settlement and rice-field classes generally increased, indicating expanding urban and agricultural land use. Pond areas fluctuated over time, while vegetation, including mangrove-associated cover, declined during several intervals. The percentage-based land-use results are emphasized because they are more robust to differences in mapping extent than absolute area values. The observed decline in vegetation during some periods is relevant to shoreline interpretation because reduced vegetated cover can lower sediment-trapping capacity and increase exposure to erosion. Therefore, the land-use results provide contextual evidence for interpreting spatial differences in shoreline behavior rather than direct inputs for DSAS rate computation.

Table 4. Land use area (ha) from 1973 to 2021

Year	Settlement	Rice Fields	Ponds	Vegetation	Rivers
1973	11,761	17,698	29,022	38,988	17,706
1982	22,284	41,557	33,063	31,296	12,504
1994	31,746	22,164	41,018	84,970	80,650
2001	31,804	29,867	31,484	98,040	75,170
2006	31,333	31,098	18,642	9,660	8,575
2011	31,889	31,885	18,611	91,062	8,843
2016	42,092	42,951	15,215	91,422	9,437
2021	40,628	43,391	18,801	95,391	8,294

Table 5. Land-use share (%) from 1973 to 2021

Year	Settlement	Rice Fields	Ponds	Vegetation	Rivers
1973	10.21	15.36	25.19	33.85	15.37
1982	15.83	29.53	23.49	22.24	8.88
1994	12.18	8.51	15.74	32.61	30.95
2001	11.94	11.21	11.82	36.81	28.22
2006	31.55	31.31	18.77	9.73	8.63
2011	17.49	17.49	10.21	49.95	4.85
2016	20.93	21.36	7.57	45.46	4.69
2021	19.67	21.01	9.10	46.19	4.02

3.3 Long-Term Shoreline Changes from 1973 to 2021

Shoreline positions from nine epochs, namely 1973, 1982, 1994, 1996, 2001, 2006, 2011, 2016, and 2021, were analyzed using DSAS across 451 transects. Area-level summaries are presented in Table 6, while the temporal and spatial patterns are shown in Figure 5 and Figure 6. Positive values indicate accretion or shoreline advance, whereas negative values indicate erosion or shoreline retreat. To ensure consistency across the 48-year observation period, EPR values were calculated as NSM divided by 48 years.

Table 6. Shoreline changes from 1973 to 2021

Area	EPR Accretion (+)	EPR Erosion (–)	EPR Net (±)	NSM Accretion (+)	NSM Erosion (–)	NSM Net (±)	Dominant
A	12.35	-5.50	+6.85	592.82	-263.85	+328.97	Accretion
B	11.54	-5.77	+5.77	553.90	-277.05	+276.85	Accretion
C	15.34	-11.10	+4.24	736.29	-532.80	+203.49	Accretion
D	8.02	-8.68	-0.66	384.76	-416.53	-31.77	Erosion
E	14.87	-4.81	+10.06	713.82	-231.00	+482.82	Accretion
F	12.45	-6.30	+6.15	597.73	-302.40	+295.33	Accretion

Note: EPR, end point rate; NSM, net shoreline movement. EPR was recomputed from NSM using EPR = NSM / ΔT, with ΔT = 48 years for the 1973–2021 observation period. Positive values indicate accretion or shoreline advance, whereas negative values indicate erosion or shoreline retreat.

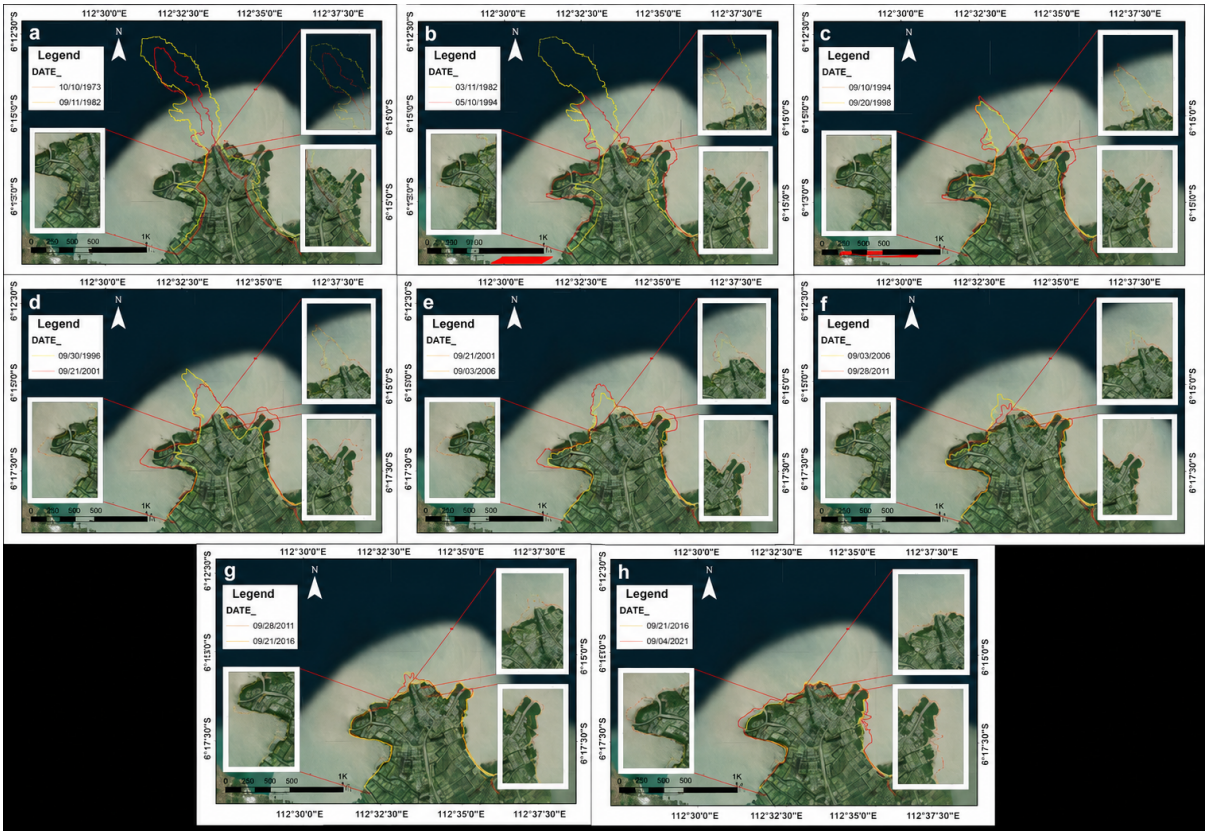

Figure 5. Temporal distribution of shoreline changes: (a) 1973–1982; (b) 1982–1994; (c) 1994–1996; (d) 1996–2001; (e) 2001–2006; (f) 2006–2011; (g) 2011–2016; and (h) 2016–2021

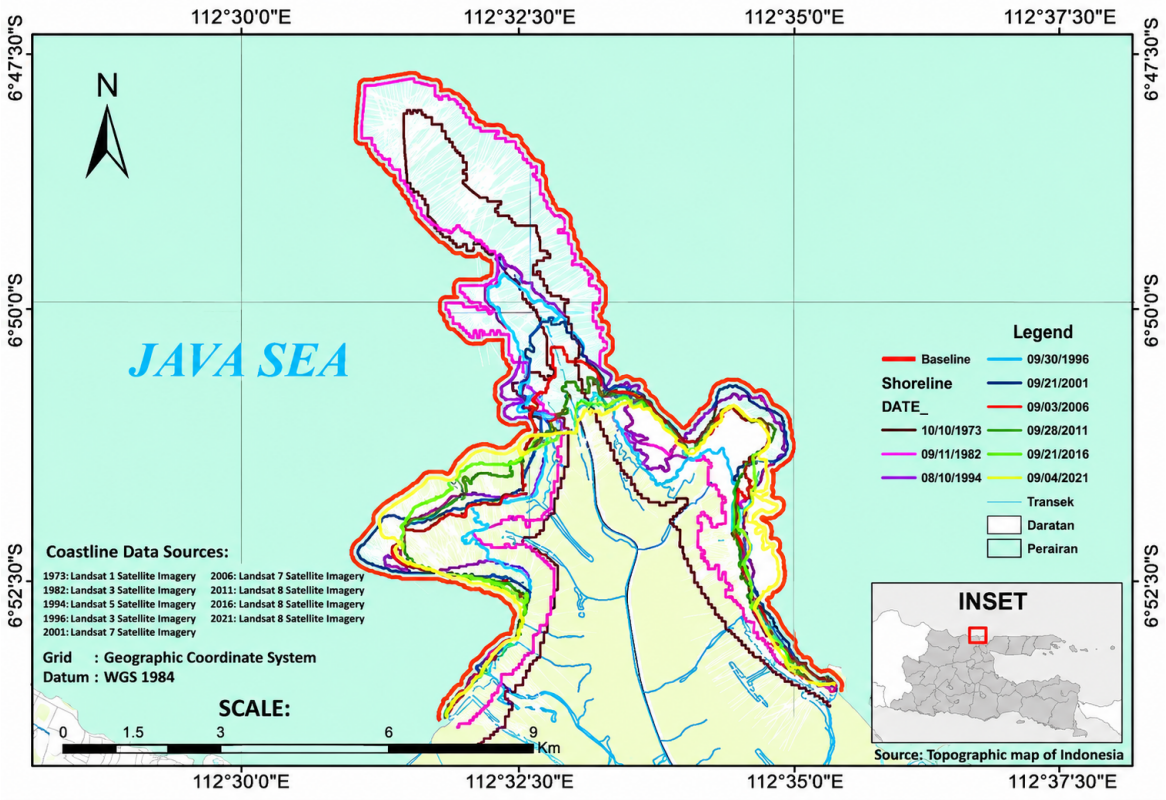

Figure 6. Map of changes in the Ujung Pangkah shoreline 1973–2021

The DSAS results show a clear spatial contrast among Areas A–F. Five areas, namely Areas A–C and E–F, were dominated by net accretion, while Area D was the only sector with net erosion (Table 6; Figure 5 and Figure 6). This pattern indicates that shoreline change in Ujung Pangkah did not occur as a uniform coast-wide trend. Instead, it formed a segment-structured mosaic of accretion and erosion.

Area-level results further clarify this spatial contrast. Area A was accretion-dominated, with average accretion of 592.82 m in NSM and 12.35 m·yr^{-1} in EPR, compared with erosion of -263.85 m in NSM and -5.50 m·yr^{-1} in EPR. Area B showed a similar accretion-dominated pattern, with accretion of 553.90 m in NSM and 11.54 m·yr^{-1} in EPR, compared with erosion of -277.05 m in NSM and -5.77 m·yr^{-1} in EPR.

Area C showed the strongest accretion signal among all sectors. This area recorded accretion of 736.29 m in NSM and 15.34 m·yr^{-1} in EPR, although erosion also occurred locally, reaching -532.80 m in NSM and -11.10 m·yr^{-1} in EPR. Area D showed the opposite pattern and formed the main erosional hotspot. It recorded erosion of -416.53 m in NSM and -8.68 m·yr^{-1} in EPR, compared with localized accretion of 384.76 m in NSM and 8.02 m·yr^{-1} in EPR. Thus, despite the presence of local accretion, the area-level signal in Area D remained erosion-dominated.

Overall, the long-term DSAS record identifies five accretion-dominated sectors and one persistent erosion sector. This spatial pattern highlights the importance of segment-scale interpretation because coast-wide averages would obscure localized erosion risk in Area D and sustained accretion gains in Areas A–C and E–F.

3.4 Ecosystem and Livelihood Impacts of Shoreline Change

The shoreline-change mosaic has important implications for mangrove habitat configuration, estuarine connectivity, and coastal livelihoods. In accretion-dominated sectors, shoreline advance can create additional accommodation space for mangrove establishment and foreshore expansion. These changes may increase habitat continuity and nearshore structural complexity, which are important for fish reproduction and juvenile nursery functions [21]. Areas A–C and E–F therefore represent sectors where accretionary gains could support mangrove maintenance or expansion if land conversion is controlled. These habitat gains are also consistent with the broader role of mangroves in coastal protection, carbon storage, and biodiversity support in deltaic environments [22, 23].

In contrast, the persistent retreat in Area D indicates a zone of shoreline instability. Erosion in this sector can reduce mangrove-edge stability, fragment habitat connectivity, and increase exposure to wave energy and sediment resuspension. These processes may weaken nursery functions for estuarine fishes and invertebrates and increase the vulnerability of pond-based livelihoods [22–24].

The contrast between accreting and eroding sectors is directly relevant to local fisheries and aquaculture systems.

Stable mangrove–estuary linkages can support ecosystem services and livelihood opportunities, whereas shoreline retreat can increase maintenance costs, habitat loss, and exposure risk for coastal communities [25, 26]. Previous studies in Ujung Pangkah and other Indonesian coastal systems have further emphasized that mangrove ecosystems support multiple management-relevant functions, including ecotourism potential, habitat-condition assessment, marine-debris monitoring, mangrove-density evaluation, and economic sustainability [27–29].

The land-use results further support this interpretation. Periodic declines in the vegetation class, including mangrove-associated cover, coincided with intervals where erosion was more evident in the shoreline-change maps (Table 4 and Table 5; Figure 5 and Figure 6). This pattern suggests a potential feedback between shoreline position, mangrove cover, and coastal exposure. It is also consistent with broader evidence that mangrove degradation can reduce natural buffering capacity and increase shoreline instability [30]. In livelihood terms, erosion can increase the vulnerability of fishers and aquaculture farmers by exposing ponds, infrastructure, and productive coastal land to recurrent losses [31].

Taken together, the results indicate two management directions. First, accretion-dominated sectors, especially Areas A–C and E–F, should be protected to maintain shoreline gains and mangrove-related ecosystem services. Second, Area D should be prioritized for targeted erosion control, mangrove rehabilitation, and livelihood-risk reduction.

4 Discussion

4.1 Comparison with Previous Studies

The shoreline-change pattern in Ujung Pangkah from 1973 to 2021 shows a stable, segment-structured contrast rather than a single coast-wide trajectory. DSAS metrics indicate that most sectors were accretion-dominated, particularly Areas A–C and E–F, where the accretion component reached approximately +12 to +15 m·yr^{-1}. In contrast, Area D formed the main erosional hotspot, with an erosion component of -8.68 m·yr^{-1} and an NSM erosion value of -416.53 m. At the area level, Area D remained erosion-dominated, with a net EPR of -0.66 m·yr^{-1} and a net NSM of -31.77 m (Table 6; Figure 5 and Figure 6). This "accretion belt + erosion pocket" pattern suggests that shoreline change in Ujung Pangkah was controlled by segment-scale differences in sediment availability, hydrodynamic exposure, and coastal land-use context. Therefore, interpreting shoreline change only from an overall mean value would obscure localized erosion risk and intervention priorities.

Comparable segment-specific shoreline behavior has been reported along the northern coast of Java using remote sensing and DSAS-based approaches. DSAS-based analysis along the Sayung–Demak coast of Central Java documented strong spatial heterogeneity in shoreline trajectories and showed that severe erosion can be concentrated in specific coastal segments, while accretion is commonly associated with local variations in waves, storm surges, tidal currents, bathymetry, and mangrove cover [32]. Similar shoreline-change studies along the Java coast also showed that coastal change can occur at rates of meters to tens of meters per year, reinforcing that the magnitudes observed in Ujung Pangkah are plausible for actively modified northern Java coastal systems [33, 34].

The Ujung Pangkah results are also consistent with local evidence from the Bengawan Solo deltaic system. Previous satellite-based assessments reported measurable progradation and land-cover transformation in the Bengawan Solo–Ujung Pangkah coastal plain, indicating a strong relationship between sediment delivery, shoreline advance, pond expansion, and mangrove or vegetation dynamics [35]. In the present study, the dominance of accretion in Areas A–C and E–F is consistent with sediment retention and delta-front development, while the persistence of erosion in Area D indicates that sediment supply and shoreline stabilization were spatially uneven.

Beyond Java, DSAS-based assessments in other deltaic environments also show that accretion and erosion frequently coexist within the same coastal system. In the Indus Delta, long-term shoreline records showed dominant retreat at the delta scale, but localized accretion pockets were still detected in specific sectors [36, 37]. A similar pattern was reported in the Meriç Delta, where erosion and accretion alternated across sub-periods and coastal segments [38]. These comparisons support the interpretation that deltaic shorelines rarely respond uniformly to regional forcing. Instead, shoreline trajectories are shaped by the local balance among sediment supply, wave–tide processes, nearshore morphology, vegetation cover, and human modification.

4.2 Scientific Implications

The DSAS results indicate that shoreline change in Ujung Pangkah is organized as a segment-structured accretion–erosion mosaic. Accretion dominated most sectors, particularly Areas A–C and E–F, whereas Area D remained the main erosional hotspot. Rather than indicating a single coast-wide trend, this pattern shows that shoreline response varied systematically alongshore. This finding is consistent with deltaic coasts where sediment retention and effective wave–current exposure are not evenly distributed among segments. Similar DSAS-based delta assessments have also reported coexisting accretion and erosion that cluster into localized hotspots over multi-decadal periods [32].

The physical setting of Ujung Pangkah helps explain this spatial sensitivity. The coast has very gentle beach slopes, ranging from approximately 0.02° to 0.05° over 1 km, with an overall mean of about 0.04° (Table 3). It is also

influenced by a diurnal tidal regime, with a Formzahl value of approximately 7.64 (Figure 4). In such a low-gradient and tide-influenced setting, even small gains or losses of sediment can produce visible shoreline displacement. The position of the waterline can also vary with tidal stage, which reinforces the need to interpret DSAS-derived shoreline changes at the segment scale.

The differences among shoreline segments can be explained by the combined influence of seasonal coastal forcing and land-use change. Monsoon-driven currents and changing wave conditions may alter the direction and intensity of alongshore sediment transport. As a result, some sectors can receive and retain more sediment, while others remain more exposed to erosion. At the same time, land-use change on the coastal plain, especially conversion between mangrove or vegetated areas and aquaculture ponds, can reduce sediment trapping and wave-buffering capacity. Similar DSAS-based studies in other deltaic systems have shown that variations in sediment supply and human modification can reinforce localized erosion and accretion, producing a persistent alongshore mosaic rather than a uniform shoreline trend [34].

These findings support the interpretation that shoreline-change metrics should not be used in isolation. DSAS provides a quantitative baseline of shoreline displacement and change rates, but hydro-oceanographic conditions, coastal slope, and land-use dynamics are needed to interpret why erosion and accretion differ among sectors. This integrated interpretation is important for deltaic environments such as Ujung Pangkah, where shoreline change reflects the combined effects of sediment supply, hydrodynamic exposure, vegetation condition, and human land use.

4.3 Management Implications

The DSAS-based spatial mosaic provides a basis for segment-specific coastal management. The results indicate strong accretionary tendencies in Areas A–C and E–F, whereas Area D showed persistent net erosion, with a net EPR of -0.66 $m \cdot yr^{-1}$ and a net NSM of -31.77 m. The erosion component in Area D reached -8.68 $m \cdot yr^{-1}$ and -416.53 m in NSM, confirming this sector as the main erosional hotspot (Table 6; Figure 5; Figure 6). Therefore, management interventions should not be applied uniformly along the coast. Accretionary sectors should be protected to maintain shoreline gains, while Area D should be prioritized for erosion control, mangrove rehabilitation, and livelihood-risk reduction.

4.3.1 Mangrove reforestation and coastal protection

Mangrove restoration should be prioritized because mangroves can reduce wave energy, enhance sediment retention, and stabilize low-gradient shorelines [39]. In Ujung Pangkah, this function is particularly important because local aquaculture expansion and vegetation changes have altered the mangrove–pond landscape [40]. Restoration should therefore be hydrology-aware, site-specific, and community-engaged to sustain both ecological and livelihood benefits [41–43].

In Area D, mangrove-based stabilization should be treated as a high-priority intervention. Restoration should focus on improving hydrologic exchange, reconnecting tidal creeks where feasible, and establishing a protective mangrove belt in areas with suitable sediment and inundation conditions. In contrast, Areas A–C and E–F should be managed to maintain accretionary gains. These areas require protection from further conversion of accreting fringes, supported by enrichment planting along prograding edges where mangrove establishment is ecologically suitable.

4.3.2 Community-based conservation

Community-based conservation can strengthen shoreline management because local fishers, pond farmers, and coastal residents are directly affected by mangrove condition and shoreline instability [44, 45]. In erosion-prone sectors, community involvement can support restoration maintenance, local monitoring, and early detection of shoreline retreat. In accreting sectors, community stewardship can help ensure that newly formed or expanding mangrove fringes are maintained as ecological assets rather than rapidly converted into ponds or other land uses.

For Area D, community-based monitoring groups could be linked with mangrove rehabilitation activities to support maintenance after planting and to document shoreline changes over time. In Areas A–C and E–F, community stewardship should focus on protecting accreting mangrove fringes so that shoreline gains translate into durable nursery habitat, coastal protection, and blue-carbon benefits [46, 47].

4.3.3 Sustainable hybrid coastal infrastructures

Hybrid coastal infrastructure may be considered where mangrove-only stabilization is insufficient. Such measures should complement nature-based rehabilitation rather than replace it. Hybrid structures can help reduce wave energy and support sediment deposition, but poorly planned hard structures can alter sediment transport and degrade coastal habitat quality [48–50].

In Ujung Pangkah, any hybrid intervention should be spatially targeted and aligned with the shoreline-change mosaic. Area D may require combined mangrove rehabilitation and low-impact supporting structures if erosion pressure remains high. However, infrastructure placement should consider seasonal current and wave patterns to avoid downdrift sediment starvation. Post-intervention monitoring should use the established remote-sensing and DSAS workflow to evaluate whether shoreline stabilization and mangrove recovery are occurring as intended.

4.3.4 Integration with spatial planning and policy alignment

The DSAS-based evidence can support spatial planning by identifying where protection, rehabilitation, and controlled-use zones should be prioritized. Area D can be designated as a rehabilitation and coastal-protection priority zone because it represents the main erosional hotspot. In contrast, Areas A–C and E–F can be managed as accretionary conservation or controlled-use zones to prevent uncontrolled conversion of newly formed coastal land.

Integrating this spatial evidence into regional coastal zoning can help reduce land-use conflicts and align shoreline-change information with mangrove management, aquaculture planning, and livelihood protection [51, 52]. Participatory implementation is also important because local compliance and long-term maintenance are more likely when community actors are involved in planning and monitoring [53]. Complementary habitat-risk screening can further support the prioritization of vulnerable areas and reinforce why Area D requires urgent intervention [54].

4.3.5 Strengthening community resilience and food security

The shoreline-change pattern has direct relevance for community resilience and food security. Accreting sectors, especially Areas C and E, provide opportunities to maintain or expand mangrove fringes that support nursery habitat and stabilize shore-adjacent aquaculture systems. These conditions may help reduce exposure and maintenance costs for pond-based livelihoods if land conversion is controlled.

In contrast, persistent retreat in Area D increases exposure of ponds, fishing infrastructure, and productive coastal land to recurrent losses. This condition supports the need to link shoreline rehabilitation with livelihood-risk reduction, aquaculture adaptation, and community resilience planning [55–57]. Therefore, coastal management in Ujung Pangkah should not only focus on shoreline stabilization, but also on protecting the ecological functions that support fisheries, aquaculture, and household income.

Taken together, these management pathways form an evidence-to-action sequence. DSAS diagnostics identify priority segments, physical and land-use datasets explain the likely drivers, and targeted interventions translate the shoreline-change evidence into coastal rehabilitation, protection, and monitoring actions. This integrated approach is consistent with social-ecological sustainability strategies for mangrove conservation, where ecological rehabilitation, community participation, and adaptive management need to be linked within a single management framework [58]. Figure 7 summarizes this evidence-to-action framework by linking the mapped shoreline-change mosaic to segment-specific management options and enabling conditions.

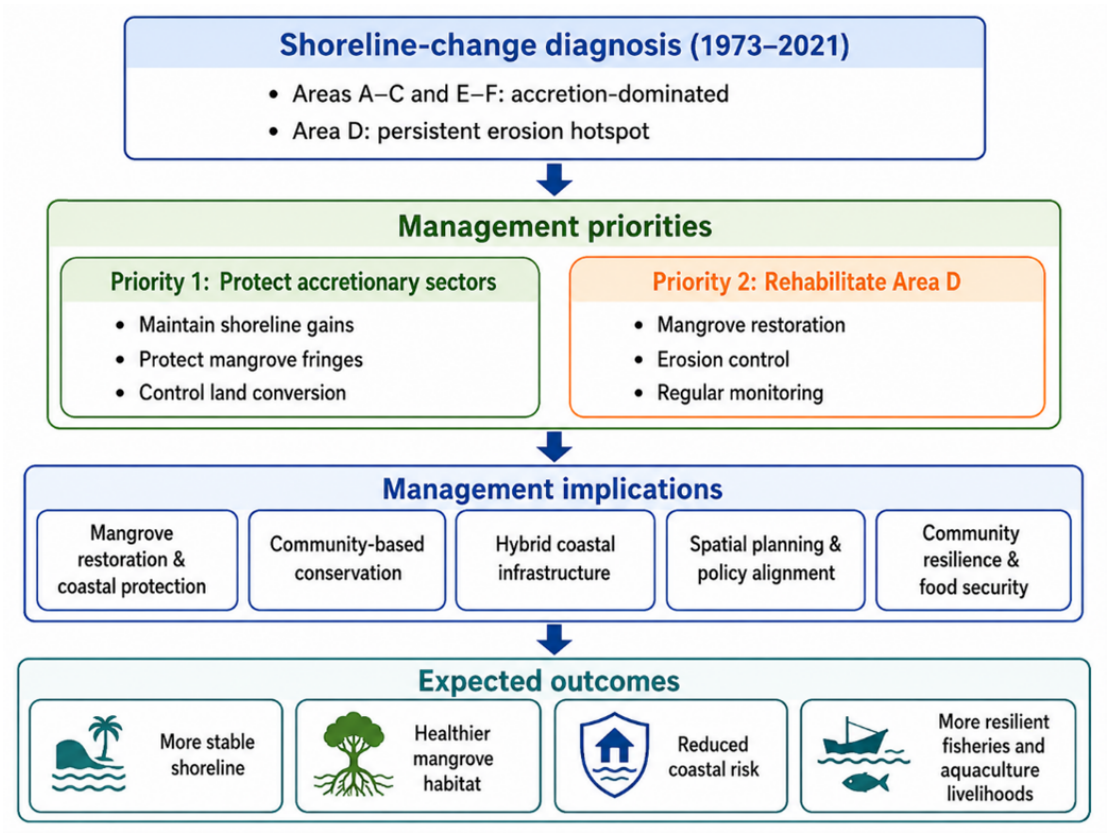

Figure 7. Management-implication framework linking shoreline-change diagnosis, priority interventions, management pathways, and expected sustainability outcomes in Ujung Pangkah

5 Conclusions

This study demonstrates that shoreline evolution in Ujung Pangkah from 1973 to 2021 was not spatially uniform but was organized as a segment-structured accretion–erosion mosaic. Most coastal sectors showed persistent accretionary tendencies, whereas Area D remained the main erosional hotspot. This finding confirms that coast-wide average shoreline-change values may obscure localized erosion risk and sustained accretion gains in dynamic deltaic environments.

The main significance of this study lies in its integration of multi-decadal satellite-derived shorelines, DSAS metrics, hydro-oceanographic context, coastal slope, and land-use information into a management-oriented assessment. This integrated workflow provides an operational baseline for identifying priority intervention zones, protecting accretionary sectors, targeting erosion control, and supporting mangrove rehabilitation and spatial-planning decisions in Ujung Pangkah.

Several limitations should be acknowledged. Shoreline extraction relied on 30-m multisensor Landsat imagery, which may introduce positional uncertainty, particularly in low-gradient and tide-influenced coastal settings. Although tidal normalization and quality-control procedures were applied, residual uncertainty related to tidal-stage variation may remain. In addition, area-level DSAS summaries may mask within-area transect variability, and land-use classification was used as contextual evidence rather than direct causal attribution.

Future research should integrate higher-resolution satellite imagery, UAV-based shoreline and mangrove-edge mapping, field validation of sediment and hydrodynamic conditions, and more detailed transect-level shoreline statistics. Post-intervention monitoring is also needed to evaluate the effectiveness of mangrove rehabilitation, hybrid coastal protection, and livelihood-oriented adaptation strategies under future coastal-management scenarios.

Author Contributions

Conceptualization, A.I. and R.; methodology, A.I., I.M.A., and D.K.S.; software, I.M.A. and D.K.S.; validation, A.I., R., A.S., T.D.L., G.B., and U.Y.; formal analysis, I.M.A. and D.K.S.; investigation, I.M.A., D.K.S., Q.A., N.R.C., A.L.F., and B.M.P.; resources, A.I., R., A.S., T.D.L., G.B., and M.M.; data curation, I.M.A., D.K.S., Q.A., and D.C.P.; writing—original draft preparation, A.I., I.M.A., and D.K.S.; writing—review and editing, A.I., R., A.S., T.D.L., G.B., U.Y., A.U., M.M., and D.C.P.; visualization, I.M.A., D.K.S., and D.C.P.; supervision, A.I., R., A.S., T.D.L., G.B., and U.Y.; project administration, A.I. All authors have read and agreed to the published version of the manuscript.

Data Availability

The data used to support the findings of this study are available from the corresponding author upon request.

Conflicts of Interest

The authors declare no conflicts of interest.

References

[1] Q. Wang, Y. Ma, Z. Cheng, and Y. Du, "Coastline changes under natural and anthropogenic drivers in a macro-tidal estuary between 2000–2020," *Front. Mar. Sci.*, vol. 10, p. 1335064, 2023. https://doi.org/10.3389/fmars.2023.1335064

[2] T. Oyedotun, A. Ruiz-Luna, and A. Navarro-Hernández, "Contemporary shoreline changes and consequences at a tropical coastal domain," *Geol. Ecol. Landscapes*, vol. 2, no. 2, pp. 104–114, 2018. https://doi.org/10.1080/24749508.2018.1452483

[3] V. D. Prasita, R. S. Bintoro, I. Nurmalia, S. Widagdo, N. Rosana, and E. Sugianto, "The coastline change pattern of Gresik Beach around the Madura Strait, Indonesia," *Indones. J. Geogr.*, vol. 55, no. 3, pp. 527–537, 2023. https://doi.org/10.22146/ijg.80934

[4] Z. Hidayah, M. Maula, and M. K. Wardhani, "Pemodelan arus dan muatan padatan tersuspensi di perairan estuari muara Bengawan Solo Ujung Pangkah Gresik," *Bul. Oseanogr. Mar.*, vol. 12, no. 1, pp. 87–97, 2023. https://doi.org/10.14710/buloma.v12i1.42322

[5] T. Worthington, P. Ermgassen, D. Friess, K. Krauss, C. Lovelock, J. Thorley, R. Tingey, C. D. Woodroffe, P. Bunting, N. Cormier, and et al., "A global biophysical typology of mangroves and its relevance for ecosystem structure and deforestation," *Sci. Rep.*, vol. 10, no. 1, p. 14652, 2020. https://doi.org/10.1038/s41598-020-71194-5

[6] N. Santoso, R. P. Nugraha, and R. Andalas, "Total economic value of mangrove forest in Pangkah Kulon and Pangkah Wetan Village Areas, Ujungpangkah District, Gresik Regency, East Java Province," *Media Konserv.*, vol. 24, no. 2, pp. 152–162, 2019. https://doi.org/10.29244/medkon.24.2.152-162

[7] M. A. Islam, M. S. Hossain, T. Hasan, and S. M. Department, "Shoreline changes along the Kutubdia Island, south east bangladesh using digital shoreline analysis system," *Bangladesh J. Sci. Res.*, vol. 27, no. 1, pp. 99–108, 2016. https://doi.org/10.3329/bjsr.v27i1.26228

[8] K. Vos, M. D. Harley, K. D. Splinter, A. Walker, and I. L. Turner, "Beach slopes from satellite-derived shorelines," *Geophys. Res. Lett.*, vol. 47, no. 14, 2020. https://doi.org/10.1029/2020GL088365

[9] T. Solihuddin, S. Husrin, H. L. Salim, T. L. Kepel, E. Mustikasari, A. Heriati, R. N. A. Ati, D. Purbani, L. O. N. Mbay, V. Y. Indriasari, and et al., "Coastal erosion on the north coast of Java: Adaptation strategies and coastal management," *IOP Conf. Ser. Earth Environ. Sci.*, vol. 777, p. 012035, 2021. https://doi.org/10.1088/1755-1315/777/1/012035

[10] Y. Du, Y. Zhang, F. Ling, Q. Wang, W. Li, and X. Li, "Water bodies' mapping from Sentinel-2 imagery with Modified Normalized Difference Water Index at 10-m spatial resolution produced by sharpening the SWIR band," *Remote Sens.*, vol. 8, no. 4, p. 354, 2016. https://doi.org/10.3390/rs8040354

[11] H. Xu, "Modification of normalised difference water index (NDWI) to enhance open water features in remotely sensed imagery," *Int. J. Remote Sens.*, vol. 27, no. 14, pp. 3025–3033, 2006. https://doi.org/10.1080/01431160600589179

[12] S. Zoysa, V. Basnayake, J. Samarasinghe, M. Gunathilake, K. Kantamaneni, N. Muttil, U. Pawar, and U. Rathnayake, "Analysis of multi-temporal shoreline changes due to a harbor using remote sensing data and GIS techniques," *Sustainability*, vol. 15, no. 9, 2023. https://doi.org/10.3390/su15097651

[13] S. Velsamy, G. Balasubramaniyan, B. Swaminathan, and D. Kesavan, "Multi-decadal shoreline change analysis in coast of Thiruchendur Taluk, Thoothukudi district, Tamil Nadu, India, using remote sensing and DSAS techniques," *Arab. J. Geosci.*, vol. 13, no. 17, 2020. https://doi.org/10.1007/S12517-020-05800-1

[14] M. Hart-Davis, D. Dettmering, R. Sulzbach, M. Thomas, C. Schwatke, and F. Seitz, "Regional evaluation of minor tidal constituents for improved estimation of ocean tides," *Remote Sens.*, vol. 13, no. 16, p. 3310, 2021. https://doi.org/10.3390/rs13163310

[15] R. Mottram, N. Hansen, C. Kittel, J. M. van Wessem, C. Agosta, C. Amory, F. Boberg, W. J. van de Berg, X. Fettweis, A. Gossart, and et al., "What is the surface mass balance of Antarctica? An intercomparison of regional climate model estimates," *Cryosphere*, vol. 15, no. 8, pp. 3751–3784, 2021. https://doi.org/10.5194/tc-15-3751-2021

[16] M. Ballarotta, C. Ubelmann, P. Veillard, P. Prandi, H. Etienne, S. Mulet, Y. Faugère, G. Dibarboure, R. Morrow, and N. Picot, "Improved global sea surface height and current maps from remote sensing and in situ observations," *Earth Syst. Sci. Data*, vol. 15, pp. 295–315, 2023. https://doi.org/10.5194/essd-15-295-2023

[17] D. Susetyo, "Vertical accuracy assessment of various open-source DEM data: DEMNAS, SRTM-1, and ASTER GDEM," *Geodesy Cartogr.*, vol. 49, no. 4, pp. 209–215, 2023. https://doi.org/10.3846/gac.2023.18168

[18] L. L. Zong, S. J. He, J. T. Lian, Q. Bie, X. Y. Wang, J. R. Dong, and Y. W. Xie, "Detailed mapping of urban land use based on multi-source data: A case study of Lanzhou," *Remote Sens.*, vol. 12, no. 12, p. 1987, 2020. https://doi.org/10.3390/rs12121987

[19] S. Aisyah, J. T. S. Sumantyo, A. Pamungkas, M. R. Muftiadi, and M. Yusuf, "A preliminary study: Marine biogeography of Nautilus in the Bangka Belitung Seas, Indonesia," *Ilmu Kelaut. Indones. J. Mar. Sci.*, vol. 26, no. 3, pp. 147–154, 2021. https://doi.org/10.14710/ik.ijms.26.3.147-154

[20] S. Toure, O. Diop, K. Kpalma, and A. Maïga, "Shoreline detection using optical remote sensing: A review," *ISPRS Int. J. Geo-Inf.*, vol. 8, no. 2, p. 75, 2019. https://doi.org/10.3390/ijgi8020075

[21] G. Sundblad and U. Bergström, "Shoreline development and degradation of coastal fish reproduction habitats," *Ambio*, vol. 43, no. 8, pp. 1020–1028, 2014. https://doi.org/10.1007/s13280-014-0522-y

[22] D. K. Saputra, B. Semedi, A. Yamindago, C. S. U. Dewi, M. A. Asadi, A. Isdianto, D. Aliviyanti, R. D. Kasitowati, A. Darmawan, A. Setyanto, and et al., "Characteristics of mangrove fisheries in essential ecosystem area Ujungpangkah, Indonesia," *J. Environ. Manag. Tour.*, vol. 13, no. 3, pp. 812–820, 2022. https://doi.org/10.14505/jemt.v13.3(59).20

[23] M. A. Asadi, G. Guntur, A. B. Ricky, P. Novianti, and A. Isdianto, "Mangrove ecosystem C-stocks of Lamongan, Indonesia and its correlation with forest age," *Res. J. Chem. Environ.*, vol. 21, no. 8, pp. 1–9, 2017.

[24] P. Bunting, L. Hilarides, A. Rosenqvist, R. M. Lucas, E. Kuto, Y. Gueye, and L. Ndiaye, "Global mangrove watch: Monthly alerts of mangrove loss for Africa," *Remote Sens.*, vol. 15, no. 8, p. 2050, 2023. https://doi.org/10.3390/rs15082050

[25] M. Troell, B. Costa-Pierce, S. Stead, R. Cottrell, C. Brugere, A. Farmery, D. C. Little, Å. Strand, R. Pullin, D. Soto, and et al., "Perspectives on aquaculture's contribution to the Sustainable Development Goals for improved human and planetary health," *J. World Aquacult. Soc.*, vol. 54, no. 2, pp. 251–342, 2023. https://doi.org/10.1111/jwas.12946

[26] B. Nagel, N. Buhari, and S. Partelow, "Archetypes of community-based pond aquaculture in Indonesia: Applying the social-ecological systems framework to examine sustainability tradeoffs," *Environ. Res. Lett.*, vol. 19, no. 4, p. 044026, 2024. https://doi.org/10.1088/1748-9326/ad2e71

[27] Z. Abidin, F. Nuryani, D. Saputra, M. Fattah, N. Harahab, and A. Kusumawati, "Mangrove potential assessment

for determining ecotourism attraction and strengthening destination branding and marketing: "Gunung Pithing Mangrove Conservation", Indonesia," *GeoJournal Tour. Geosites*, vol. 47, no. 2, pp. 388–396, 2023. https://doi.org/10.30892/gtg.47204-1036

[28] N. F. F. Ramadhanti, A. L. Fathah, M. N. E. Putra, B. M. Putri, and A. Isdianto, "Non-destructive transect assessment of marine debris and mangrove density in urban mangrove ecosystems," *Eng. Technol. Appl. Sci. Res.*, vol. 15, no. 6, pp. 29 810–29 815, 2025. https://doi.org/10.48084/etasr.13930

[29] M. Primyastanto, M. P. Wardani, S. Supriyadi, S. K. A. Nisa', E. D. Nadila, and A. F. A. Mazaya, "Analysis of total economic value as a key to sustainability of the mangrove ecosystem of Permata Pilang Probolinggo," *Int. J. Environ. Impacts*, vol. 8, no. 6, pp. 1206–1221, 2025. https://doi.org/10.56578/ijei080608

[30] M. Besset, N. Gratiot, E. J. Anthony, F. Bouchette, M. Goichot, and P. Marchesiello, "Mangroves and shoreline erosion in the Mekong River delta, Viet Nam," *Estuar. Coast. Shelf Sci.*, vol. 226, p. 106263, 2019. https://doi.org/10.1016/j.ecss.2019.106263

[31] E. W. Riptanti, M. Harisudin, K. Kusnandar, I. Khomah, N. Setyowati, A. Qonita, R. W. Nugroho, and S. Gayatri, "The effect of abrasion on resilience of fishermen/fish farmer livelihoods on the North Coast of Central Java," *Edelweiss Appl. Sci. Technol.*, vol. 8, no. 6, pp. 1882–1894, 2024. https://doi.org/10.55214/25768484.v8i6.2354

[32] M. R. Muskananfola, Supriharyono, and S. Febrianto, "Spatio-temporal analysis of shoreline change along the coast of Sayung Demak, Indonesia using Digital Shoreline Analysis System," *Reg. Stud. Mar. Sci.*, vol. 34, p. 101060, 2020. https://doi.org/10.1016/j.rsma.2020.101060

[33] N. Khakhim, A. Kurniawan, W. S. Pranowo, E. U. Khasanah, and P. Halilintar, "Shoreline morphological change prognostic model based on spatiotemporal framework imagery data on the northern coast of Java, Indonesia," *Kuwait J. Sci.*, vol. 51, no. 4, p. 100274, 2024. https://doi.org/10.1016/j.kjs.2024.100274

[34] S. Arjasakusuma, S. S. Kusuma, S. Saringatin, P. Wicaksono, B. W. Mutaqin, and R. Rafif, "Shoreline dynamics in East Java Province, Indonesia, from 2000 to 2019 using multi-sensor remote sensing data," *Land*, vol. 10, no. 2, p. 100, 2021. https://doi.org/10.3390/land10020100

[35] A. Sartimbul, S. W. Ningtias, C. S. U. Dewi, M. A. A. Rahman, D. Yona, S. H. J. Sari, and N. Hidayati, "Monitoring of sedimentation on geosynthetic bags installation area in Banyuurip Mangrove Center, Ujung Pangkah, Gresik, Indonesia," *Ilmu Kelaut. Indones. J. Mar. Sci.*, vol. 26, no. 3, pp. 173–181, 2021. https://doi.org/10.14710/ik.ijms.26.3.173-181

[36] H. Batool, Z. He, N. A. Kalhoro, and X. Kong, "Geospatial analysis of shoreline shifts in the Indus Delta using DSAS and satellite data," *J. Mar. Sci. Eng.*, vol. 13, no. 10, p. 1986, 2025. https://doi.org/10.3390/jmse13101986

[37] A. Siyal, G. Solangi, Z. Siyal, P. Siyal, M. Babar, and K. Ansari, "Shoreline change assessment of Indus Delta using GIS-DSAS and satellite data," *Reg. Stud. Mar. Sci.*, vol. 53, p. 102405, 2022. https://doi.org/10.1016/j.rsma.2022.102405

[38] H. Kılar, "Shoreline change assessment using DSAS technique: A case study on the coast of Meriç Delta (NW Türkiye)," *Reg. Stud. Mar. Sci.*, vol. 57, p. 102737, 2023. https://doi.org/10.1016/j.rsma.2022.102737

[39] H. L. Hayden and E. F. Granek, "Coastal sediment elevation change following anthropogenic mangrove clearing," *Estuar. Coast. Shelf Sci.*, vol. 165, pp. 70–74, 2015. https://doi.org/10.1016/j.ecss.2015.09.004

[40] C. Muryani and D. Ni'matussyahara, "The area and distribution changes of mangrove forests on the coast of Gresik Regency, East Java, 2012–2023," *IOP Conf. Ser. Earth Environ. Sci.*, vol. 1357, no. 1, p. 012026, 2024. https://doi.org/10.1088/1755-1315/1357/1/012026

[41] R. Safe'i and A. N. Syahiib, "Optimization of mangrove ecosystem services based on comparison of stand carbon stock estimates in climate change mitigation," *Int. J. Environ. Impacts*, vol. 6, no. 4, pp. 197–205, 2023. https://doi.org/10.18280/ijei.060404

[42] R. Rudianto, V. Darmawan, A. Isdianto, and G. Bintoro, "Restoration of coastal ecosystems as an approach to the integrated mangrove ecosystem management and mitigation and adaptation to climate changes in north coast of East Java," *J. Coast. Conserv.*, vol. 26, no. 4, p. 37, 2022. https://doi.org/10.1007/s11852-022-00865-4

[43] Rudianto, N. Nurdiana, and A. Isdianto, "Trends and challenges of mangrove restoration management—A lessons from Labuhan Village, Indonesia," *Ecol. Environ. Conserv.*, vol. 25, no. 2, pp. 938–946, 2019.

[44] U. Muneenam, N. Bamroongragsa, D. Khahong, H. Lemkatem, and R. Tongyoi, "Local people's perception of a mangrove forest plantation as a carbon sink, Chumphon Islands National Park, Thailand," *Int. J. Environ. Impacts*, vol. 8, no. 2, pp. 277–287, 2025. https://doi.org/10.18280/ijei.080208

[45] P. Budiono, C. Wulandari, A. P. Apriliani, and F. Y. Sari, "The impact of village governance environmental management on community-based mangrove development in Karang City, Bandar Lampung," *Int. J. Environ. Impacts*, vol. 7, no. 4, pp. 675–683, 2024. https://doi.org/10.18280/ijei.070408

[46] A. L. Fathah, B. Semedi, F. C. Wardana, and A. Isdianto, "Non-destructive estimation of mangrove carbon for blue carbon accounting in data-limited regions," *Eng. Technol. Appl. Sci. Res.*, vol. 15, no. 5, pp. 27 112–27 118, 2025. https://doi.org/10.48084/etasr.12732

[47] A. L. Fathah, B. Semedi, F. C. Wardana, and A. Isdianto, "Remote sensing-based estimation of mangrove Above-Ground Carbon using Sentinel-2 vegetation indices and Random Forest," *Eng. Technol. Appl. Sci. Res.*, vol. 15, no. 6, pp. 29 598–29 604, 2025. https://doi.org/10.48084/etasr.14335

[48] G. Caldera, J. Stolle, D. P. Van Bang, A. Cornett, E. Murphy, and I. Nistor, "Wave attenuation of saltmarsh vegetation under storm conditions," *Coast. Eng. Proc.*, no. 37, p. 26, 2023. https://doi.org/10.9753/icce.v37.management.26

[49] A. E. Sutton-Grier, K. Wowk, and H. Bamford, "Future of our coasts: The potential for natural and hybrid infrastructure to enhance the resilience of our coastal communities, economies and ecosystems," *Environ. Sci. Policy*, vol. 51, pp. 137–148, 2015. https://doi.org/10.1016/j.envsci.2015.04.006

[50] R. K. Gittman, S. B. Scyphers, C. J. Baillie, A. Brodmerkel, J. H. Grabowski, M. Livernois, A. K. Poray, C. S. Smith, and F. J. Fodrie, "Reversing a tyranny of cascading shoreline-protection decisions driving coastal habitat loss," *Conserv. Sci. Pract.*, vol. 3, no. 9, p. e490, 2021. https://doi.org/10.1111/csp2.490

[51] A. Isdianto, A. L. Fathah, M. N. E. Putra, and B. M. Putri, "Geospatial change detection of mangrove loss, persistence, and regeneration in Lombok Island, Indonesia (2019–2024) using geomatic technologies," *Eng. Technol. Appl. Sci. Res.*, vol. 16, no. 2, pp. 34 270–34 275, 2026. https://doi.org/10.48084/etasr.13896

[52] R. Achmad Djazuli, G. S. Tanjung, K. Ramadhani, and M. A. Lutf, "Strategy for optimizing coastal village communities in supporting the protection of essential ecosystem areas in Gresik Regency," *Agric. Sci.*, vol. 5, no. 1, pp. 13–30, 2021. https://doi.org/10.55173/agriscience.v5i1.6

[53] E. Susilo, A. Isdianto, I. N. Y. Parawangsa, A. L. Fathah, and B. M. Putri, "Balancing tradition and conservation: The use of turtles in balinese ceremonies and its environmental implications," *Int. J. Environ. Impacts*, vol. 7, no. 2, pp. 233–243, 2024. https://doi.org/10.18280/ijei.070208

[54] K. K. Arkema, G. Verutes, J. R. Bernhardt, C. Clarke, S. Rosado, M. Canto, S. A. Wood, M. Ruckelshaus, A. Rosenthal, M. McField, and J. de Zegher, "Assessing habitat risk from human activities to inform coastal and marine spatial planning: A demonstration in Belize," *Environ. Res. Lett.*, vol. 9, no. 11, p. 114016, 2014. https://doi.org/10.1088/1748-9326/9/11/114016

[55] B. K. van Wesenbeeck, T. Balke, P. van Eijk, F. Tonneijck, M. Sirye, M. E. Rudiantoe, and J. C. Winterwerp, "Aquaculture induced erosion of tropical coastlines throws coastal communities back into poverty," *Ocean Coast. Manag.*, vol. 116, pp. 466–469, 2015. https://doi.org/10.1016/j.ocecoaman.2015.09.004

[56] P. Glassey, "How future sea level rise will affect south Dunedin," *Int. J. Environ. Impacts*, vol. 1, no. 1, pp. 40–49, 2018. https://doi.org/10.2495/ei-v1-n1-40-49

[57] S. Putiamini, M. Mulyani, M. P. Patria, T. E. B. Soesilo, and A. Karsidi, "Social vulnerability of coastal fish farming community to tidal rob flooding: A case study from Indramayu, Indonesia," *J. Coast. Conserv.*, vol. 26, no. 2, p. 7, 2022. https://doi.org/10.1007/s11852-022-00854-7

[58] Yulma, A. Kustanti, Soemarno, and M. Mahmudi, "Sustainability strategy for mangrove and crab conservation in Tarakan, Indonesia: A social-ecological system approach," *Int. J. Environ. Impacts*, vol. 8, no. 5, pp. 899–906, 2025. https://doi.org/10.56578/ijei080506